# Theoretical investigation of polarization-insensitive data format conversion of RZ-OOK to RZ-BPSK in a nonlinear birefringent fiber

**C. C. Wei[1, 2, 3], W. Astar[1, 4], J. Chen[3*], Y.-J. Chen[2], and G. M. Carter[1, 2]**

*[1]The Laboratory for Physical Sciences (LPS), 8050 Greenmead Drive, College Park, MD 20740, USA*
*[2]Department of Computer Science and Electrical Engineering, University of Maryland Baltimore County (UMBC), 1000 Hilltop Circle, Baltimore, MD 21250, USA*
*[3]Institute of Electro-Optical Engineering and Department of Photonics, National Chiao Tung University, 1001 Ta Hsueh Rd., Hsin-Chu, Taiwan, 300*
*[4]The Center for Advanced Studies in Photonics Research (CASPR), 1000 Hilltop Circle, Baltimore, MD 21250, USA*
*[*]Corresponding author: jchen@mail.nctu.edu.tw*

**Abstract:** Polarization-insensitive conversion of return-to-zero (RZ) ON-OFF keying (RZ-OOK) to RZ binary phase-shift keying (RZ-BPSK) has been achieved by cross-phase modulation (XPM) in a nonlinear birefringent fiber. This work presents a theoretical analysis of the dependence of format conversion on pump-probe detuning, and the pump state-of-polarization (SOP) that can fluctuate unpredictably in a realistic system. An investigation of the impact of pump polarization fluctuation on receiver sensitivity and receiver optimal threshold for the converted RZ-BPSK probe is also carried out. It was found that although the desired XPM-induced $\pi$ phase shift can be achieved by launching both the RZ-OOK pump and the probe along the same birefringent axis of the fiber, the phase shift degrades to $\pi/3$ if the SOP of the RZ-OOK pump unpredictably switches to the other axis of the fiber, resulting in a large receiver sensitivity penalty fluctuation of 14 dB. By contrast, launching the probe at $45^{\circ}$ relative to the birefringent axes can reduce the polarization-dependent receiver sensitivity penalty fluctuation to about 2 dB as the SOP of the RZ-OOK pump is swept over the Poincaré sphere. These conclusions are in good agreement with recently published experimental results.



**OCIS codes:** (060.5060) Phase Modulation; (070.4340) Nonlinear optical signal processing; (190.4370) Nonlinear optics, fibers; (260.1440) Birefringence

## References and links

1. A. H. Gnauck and P. J. Winzer, "Optical phase-shift-keyed transmission," J. Lightwave Technol. **23**, 115–130 (2005).
2. K. Mishina, A. Maruta, S. Mitani, T. Miyahara, K. Ishida, K. Shimizu, T. Hatta, K. Motoshima, and K.-I. Kitayama, "NRZ-OOK-to-RZ-BPSK modulation-format conversion using SOA-MZI wavelength converter," J. Lightwave Technol. **24**, 3751–3758 (2006).
3. W. Astar, A. S. Lenihan, and G. M. Carter, "Performance of DBPSK in a 5 × 10 Gb/s mixed modulation format Raman/EDFA WDM system," IEEE Photon. Technol. Lett. **17**, 2766–2768 (2005).
4. W. Astar and G. M. Carter, "10 Gbit/s RZ-OOK to RZ-BPSK format conversion using SOA and synchronous pulse carver," Electron. Lett. **44**, 369–370 (2008).
5. Cishuo Yan, Yikai Su, Lilin Yi, Lufeng Leng, Xiangqing Tian, Xinyu Vu, and Yue Tian, "All-optical format conversion from NRZ to BPSK using a single saturated SOA," IEEE Photon. Technol. Lett. **18**, 2368–2370 (2006).
6. H. Jiang, He Wen, Liuyan Han, Yili Guo, and Hanyi Zhang, "All-optical NRZ-OOK to BPSK format conversion in an SOA-based nonlinear polarization switch," IEEE Photon. Technol. Lett. **19**, 1985–1987 (2007).

#106045 - $15.00 USD Received 6 Jan 2009; revised 23 Feb 2009; accepted 24 Feb 2009; published 3 Mar 2009

7. K. Mishina, S. Kitagawa, and A. Maruta, "All-optical modulation format conversion from on-off-keying to multiple-level phase-shift-keying based on nonlinearity in optical fiber," Opt. Express **15**, 8444–8453 (2007), http://www.opticsexpress.org/abstract.cfm?uri=OE-15-13-8444.
8. W. Astar, C.-C. Wei, Y.-J. Chen, J. Chen, and G. M. Carter, "Polarization-insensitive, 40 Gb/s wavelength and RZ-OOK-to-RZ-BPSK modulation format conversion by XPM in a highly nonlinear PCF," Opt. Express **16**, 12039–12049 (2008), http://www.opticsinfobase.org/abstract.cfm?URI=oe-16-16-12039.
9. S. Kumar, A. Selvarajan, and G. Anand, "Nonlinear propagation of two optical pulses of two different frequencies in birefringent fibers," J. Opt. Soc. Am. B **11**, 810–817 (1994).
10. G. P. Agrawal, *Nonlinear Fiber Optics* (Academic Press, San Diego, CA, 2001), Chap. 7.
11. D. Marcuse, "Derivation of analytical expressions for the bit-error probability in lightwave systems with optical amplifiers," J. Lightwave Technol. **8**, 1819–1826 (1990).
12. E. W. Weisstein, "Noncentral Chi-Squared Distribution." From MathWorld--A Wolfram Web Resource. http://mathworld.wolfram.com/NoncentralChi-SquaredDistribution.html.
13. S. Stein, "Unified analysis of certain coherent and noncoherent binary communications systems," IEEE. Trans. Info. Theory **10**, 43–51 (1964).
14. K.-P. Ho, *Phase-Modulated Optical Communication System* (Springer, 2005), Appendix 3.A.

## 1. Introduction

Compared with traditional RZ-OOK, RZ differential phase-shift keying (RZ-DPSK) requires about 3-dB lower optical signal-to-noise ratio (OSNR) to achieve the same bit-error rate (BER), but a more complex transmitter and receiver [1]. The RZ-DPSK and RZ-OOK formats can fit different networks [2], and mixed RZ-OOK/RZ-DPSK transmission in wavelength division multiplexed (WDM) systems could happen through optical cross-connects (OXC) interconnecting different networks. However, RZ-OOK can seriously distort RZ-DPSK by cross-phase modulation (XPM) [3], but this impairment may be mitigated by implementing RZ-OOK-to-RZ-BPSK format conversion at the OXC level. All-optical RZ-OOK-to-RZ-BPSK format conversion has been carried out by the XPM effect in nonlinear media, such as semiconductor optical amplifiers (SOAs) [2, 4-6] and highly nonlinear fibers (HNLFs) [7]. Although the ultra-fast $\chi^{(3)}$ effect in an HNLF can achieve high speed conversion unlike a SOA limited by a slow response time, the $\chi^{(3)}$ effect is polarization-sensitive and the strength of the XPM effect induced by arbitrarily polarized RZ-OOK signals would fluctuate unpredictably. Recently, the XPM effect in a linearly birefringent photonic crystal fiber (PCF) has been proposed to achieve polarization-insensitive RZ-OOK-to-BPSK conversion [8]. In this scheme, the local probe beam is launched equally to both birefringent axes of the fiber to reduce polarization sensitivity, obviating the necessity of sophisticated and costly polarization tracking of the RZ-OOK signal. To further study the polarization sensitivity, a theoretical analysis on the format conversion in a linearly birefringent HNLF is presented here for the first time. The penalty induced by insufficient XPM-induced phase shift is also analytically investigated.

## 2. The XPM effect in a birefringent fiber

As shown in Fig. 1, while a space in an RZ-OOK signal induces negligible phase shift (close to zero), a mark with specific power is supposed to generate a $\pi$ phase shift to realize all-optical RZ-OOK-to-BPSK conversion. In the conversion process, the pulse width of the RZ-OOK signal is normally required to be broader than that of the probe beam to reduce unnecessary chirping. Moreover, to avoid erroneous reception of the RZ-BPSK signal in a direct-detection DPSK receiver, an electronic decoder would be required in the receiver as noted by Mishina *et al.* [2].

#106045 - $15.00 USD Received 6 Jan 2009; revised 23 Feb 2009; accepted 24 Feb 2009; published 3 Mar 2009

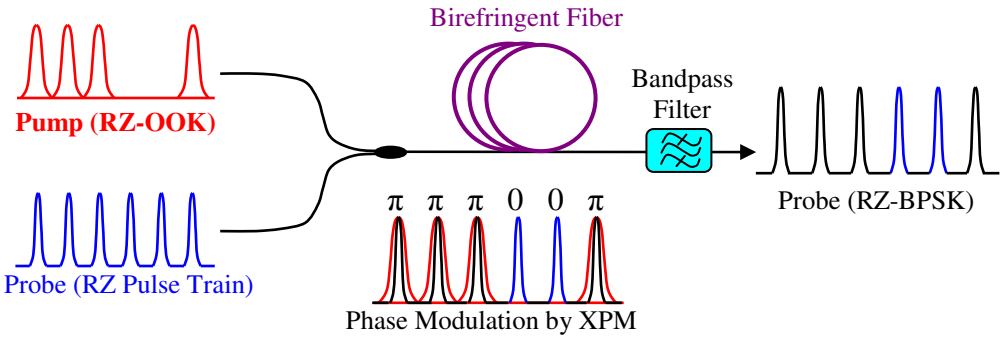


Fig. 1. RZ-OOK-to-RZ-BPSK format conversion in a birefringent fiber.

To investigate the polarization-dependent XPM effect, it is assumed that $\chi^{(3)}_{xxyy} = \chi^{(3)}_{xyxy} = \chi^{(3)}_{xyyx} = \chi^{(3)}_{xxxx}/3$, so that the third order nonlinear effect in a linearly birefringent HNLF is described by the nonlinear Schrödinger Eqs. (NLSE) [9, 10],

$$\frac{dA_{mp}}{dz} = j\gamma(|A_{mp}|^2 + 2|A_{np}|^2 + \frac{2}{3}|A_{mq}|^2 + \frac{2}{3}|A_{nq}|^2)A_{mp} + j\frac{\gamma}{3}A^*_{mp}A^2_{mq}e^{-j2\Delta\beta_{mpq}z} + j\frac{2\gamma}{3}A^*_{np}A_{nq}A_{mq}e^{-j(\Delta\beta_{mpq}+\Delta\beta_{npq})z} + j\frac{2\gamma}{3}A_{np}A^*_{nq}A_{mq}e^{-j(\Delta\beta_{mpq}-\Delta\beta_{npq})z}, \quad (1)$$

where the subscripts $m \in \{1,2\}$ and $n \in \{1,2\}$ such that $m \neq n$ refer to either the RZ-OOK pump ($m$ or $n = 1$), or the RZ pulse probe ($m$ or $n = 2$); the subscripts $p \in \{x, y\}$ and $q \in \{x, y\}$ such that $p \neq q$ represent two birefringent axes of the fiber; $A_{mp}$ is the amplitude of the electrical field; $\gamma$ is the nonlinear coefficient, and $\Delta\beta_{mpq} = \beta_{mp} - \beta_{mq}$ is the wave-vector mismatch due to the linear birefringence of the fiber. In Eq. (1), the retarded time frame has been adopted, and the dispersion and loss have been neglected assuming that the fiber length $L$ is such that $L \cong L_{eff} = (1-e^{-\alpha L})/\alpha$ and $L << L_D = T_0^2/|\beta''|$, where $L_{eff}$, $L_D$, $\alpha$, $T_0$ and $\beta''$ respectively are the effective length, the dispersion length, the fiber attenuation, the input pulse width and the group-velocity dispersion parameter. In Eq. (1), the principal axes are assumed to coincide with the birefringent axes of the fiber. Because the probe beam is a RZ pulse train, its launch power has to be sufficiently low to reduce the undesirable self-phase modulation effect. Besides, since most high ($10^{-5}$-$10^{-3}$) linear-birefringence fibers can satisfy the condition of $L|\Delta\beta_{mpq}| >> 2\pi$, the second and third terms in the RHS of Eq. (1) frequently change signs so that their contributions can be neglected [9]. Hence, the NLSEs for the pump and probe fields reduce to the following,

$$\frac{dA_{1p}}{dz} = j\gamma(|A_{1p}|^2 + \frac{2}{3}|A_{1q}|^2)A_{1p}, \quad (2)$$

$$\frac{dA_{2p}}{dz} = j\gamma(2|A_{1p}|^2 + \frac{2}{3}|A_{1q}|^2)A_{2p} + j\frac{2\gamma}{3}A_{1p}A^*_{1q}A_{2q}e^{j(\Delta\beta_{1pq}-\Delta\beta_{2pq})z}. \quad (3)$$

If the peak power of the pump beam is $P_1$, its field can be represented as $\mathbf{A}_1(z=0) = \sqrt{P_1}\cos\psi_1 e^{j\theta_{1x}}\hat{\mathbf{x}} + \sqrt{P_1}\sin\psi_1 e^{j\theta_{1y}}\hat{\mathbf{y}}$, where $\psi_1$ ($\in[0,\pi/2]$) and $\theta_1$ collectively determine the SOP of the launched pump beam. The corresponding solutions to Eq. (2) are,

#106045 - $15.00 USD Received 6 Jan 2009; revised 23 Feb 2009; accepted 24 Feb 2009; published 3 Mar 2009

$$A_{1x}(z) = A_{1x}(0)\exp\left[ j\frac{\gamma P_1}{3}\left(2+\cos^2\psi_1\right)z \right], \tag{4}$$

$$A_{1y}(z) = A_{1y}(0)\exp\left[ j\frac{\gamma P_1}{3}\left(2+\sin^2\psi_1\right)z \right]. \tag{5}$$

After using Eqs. (4) and (5), setting $\tilde{A}_{2x} = A_{2x}\exp(j\kappa z)$ and $\tilde{A}_{2y} = A_{2y}\exp(-j\kappa z)$ with $\kappa = \Delta\beta_{1xy} - \Delta\beta_{2xy} - \gamma P_1\cos(2\psi_1)/3$ in Eq. (3), Eq.(3) is then differentiated into a second-order homogenous ordinary differential equation that may be subsequently solved for $\tilde{A}_{2x}$ and $\tilde{A}_{2y}$. If the input probe is represented as $\mathbf{A}_2(z=0) = \sqrt{P_2}\cos\psi_2\, e^{j\theta_{2x}}\hat{\mathbf{x}} + \sqrt{P_2}\sin\psi_2\, e^{j\theta_{2y}}\hat{\mathbf{y}}$, the output probe becomes,

$$A_{2x}(L) = A_{2x}(0)\left[ \cos\left(\frac{kL}{2}\right) + j\,\mu_x \sin\left(\frac{kL}{2}\right)\right]\exp\left[ j\left(\frac{3\gamma P_1}{2} - j\frac{\gamma P_1}{3}\sin^2\psi_1 - j\frac{\Delta\mathrm{K}}{2}\right)L \right], \tag{6}$$

$$A_{2y}(L) = A_{2y}(0)\left[ \cos\left(\frac{kL}{2}\right) + j\,\mu_y \sin\left(\frac{kL}{2}\right)\right]\exp\left[ j\left(\frac{3\gamma P_1}{2} - j\frac{\gamma P_1}{3}\cos^2\psi_1 + j\frac{\Delta\mathrm{K}}{2}\right)L \right], \tag{7}$$

where

$$k = \sqrt{\frac{4}{9}\gamma^2 P_1^2\sin^2(2\psi_1) + [\gamma P_1\cos(2\psi_1) + \Delta\mathrm{K}]^2}\,, \tag{8}$$

$$\mu_x = \frac{1}{k}\left[ \gamma P_1\cos(2\psi_1) + \Delta\mathrm{K} + \frac{2\gamma P_1}{3}\tan\psi_2\sin(2\psi_1)\, e^{j\Delta\theta} \right], \tag{9}$$

$$\mu_y = \frac{1}{k}\left[ -\gamma P_1\cos(2\psi_1) - \Delta\mathrm{K} + \frac{2\gamma P_1}{3}\cot\psi_2\sin(2\psi_1)\, e^{-j\Delta\theta} \right], \tag{10}$$

$\Delta\theta = \theta_{1x} - \theta_{1y} - \theta_{2x} + \theta_{2y}$ is the differential phase that derives from the launch SOPs of the pump and the probe, and $\Delta\mathrm{K} = \Delta\beta_{1xy} - \Delta\beta_{2xy}$ is the differential wave-vector mismatch, which is dependent on the fiber phase-index birefringence and pump-probe detuning (PPD, $\Delta\lambda = \lambda_1 - \lambda_2$) [8]. Although $|A_{2p}(L)|^2$ may not be equal to $|A_{2p}(0)|^2$ due to the last term of Eq. (3) being complex, the total power is unchanged, i.e. $|\mathbf{A}_2(L)|^2 = P_2$. Furthermore, because the nonlinear phase shifts induced in $A_{2x}(L)$ and $A_{2y}(L)$ are not the same, an effective phase shift is needed to investigate polarization-dependent effects. Considering differential balanced direct-detection, the detected signal will be proportional to $|E(t)E^*(t-T)|\cos(\Delta\phi + \xi_0)$, where $E(t)$ is the optical field; $T$ is the bit period, and $\Delta\phi$ is the phase difference between $E(t)$ and $E(t-T)$. Additional phase-shift ($\xi_0$) in the receiver Mach-Zehnder interferometer may favorably influence the performance of the received signal, but for the ensuing analysis, it is set to zero as it would be for a standard RZ-DPSK signal expected by the receiver (thus, the converted probe would be analyzed under the same conditions as the baseline signal.) When the phase shift induced by the space of the RZ-OOK pump is zero, the effective XPM-induced phase shift of Eqs. (6) and (7) can be evaluated as,

#106045 - $15.00 USD Received 6 Jan 2009; revised 23 Feb 2009; accepted 24 Feb 2009; published 3 Mar 2009

$$\phi_{eff} = \cos^{-1}\left(\frac{|A_{2x}(0)A_{2x}(L)|\cos\phi_x + |A_{2y}(0)A_{2y}(L)|\cos\phi_y}{|A_{2x}(0)|^2 + |A_{2y}(0)|^2}\right), \quad (11)$$

where $\phi_x = \arg\{A_{2x}(L)/A_{2x}(0)\}$ and $\phi_y = \arg\{A_{2y}(L)/A_{2y}(0)\}$ are the nonlinear phase shifts of the probe field components. In general, the effective phase shift $\phi_{eff}$ is a function of $\psi_1$, $\psi_2$, $\Delta\theta$, and $\Delta$K. When the RZ-OOK pump is arbitrarily polarized, $\psi_1$ and $\Delta\theta$ become random. To focus on optimizing the controllable SOP of the probe, $L|\Delta\text{K}| >> 2\pi$ is assumed. Therefore, the last term of Eq. (3) can be neglected, and the effective phase shift becomes,

$$\phi_{eff} = \cos^{-1}\left(\cos^2\psi_2 \cos\left(\frac{\Phi(1+2\cos^2\psi_1)}{3}\right) + \sin^2\psi_2 \cos\left(\frac{\Phi(1+2\sin^2\psi_1)}{3}\right)\right), \quad (12)$$

where $\Phi$ $(= 2\gamma P_1 L)$ is termed the nonlinear phase shift due to XPM. Equations (11) and (12) reveal a complex relationship between the nonlinear phase shift ($\Phi$), and the actual effective phase-shift ($\phi_{eff}$) acquired by a probe pulse in the interaction with the pump in the fiber. It can be seen that Eq. (12) degenerates to the nonlinear phase shift *if* the pump and the probe are *both* launched along either birefringent axes.

Figure 2(a) shows an animation of $\phi_{eff}$ as a function of $\psi_2$ (Eq. (12)), under the constraints of $L|\Delta\text{K}| >> 2\pi$ and $\Phi = \pi$, where multiple curves correspond to all possible pump SOPs. Since $\phi_{eff}$ in Eq. (12) is independent of $\Delta\theta$, pump SOPs lying on identical $S_1$ planes on the Poincaré sphere induce the same $\phi_{eff}$ in Fig. 2(a). Although launching the probe along a birefringent axis ($\psi_2 = 0$) can achieve the desired $\phi_{eff} = \pi$ at one pump SOP ($\psi_1 = 0$), as the pump SOP is varied, this probe orientation results in the largest fluctuation ($\sim 2\pi/3$) in $\phi_{eff}$, i.e. with a minimum $\phi_{eff}$ of $\pi/3$ and a maximum $\phi_{eff}$ of $\pi$. By contrast, although launching the probe at $\pi/4$ relative to a principal axes sacrifices some nonlinear phase shift, as the pump SOP is varied, this probe orientation leads to the smallest fluctuation ($< \pi/10$) in $\phi_{eff}$, with a minimum of ~0.58π, and a maximum of ~0.67π. In fact, it can be observed from Fig. 2(a) that a probe launch of π/4 yields the global optimum for $\phi_{eff}$ fluctuations. In order to analyze the PPD-dependence of the fluctuations of $\phi_{eff}$ for variable pump SOP, $\psi_2 = \pi/4$ is now defined as the best scenario, while $\psi_2 = 0$ (or $\pi/2$), the worst scenario. An animation of $\phi_{eff}$ for the best scenario (with $\Phi = \pi$) is plotted as a function of $L|\Delta\text{K}|$ in Fig. 2(b), where the maximum and minimum effective phase shifts of the worst scenario are also shown for comparison. At $L|\Delta\text{K}| = 2N\pi$ (*N,* a positive integer), the minimum phase fluctuations are achieved; because the last term of Eq. (3) contributes least. In fact, for $L|\Delta\text{K}| \geq 2\pi$, the minimum phase shift remains about the same, while the phase fluctuation changes by no more than 0.02 radians. Hence, polarization-insensitive operation can be achieved by launching the probe at $\pi/4$ and requiring $L|\Delta\text{K}| \geq 2\pi$. Using experimental data from [8], a 30-m commercial PCF (NL-1550-NEG-1 fabricated by Crystal Fibre A/S) has $L_{eff}$ of 29.2 m ($\cong L$ for $\alpha = 8\times10^{-3}$ dB/m) and $L_D$ of 1 km ($>> L$ for $T_0$ = 1.13 ps, $\beta'' = 1.27$ ps$^2$/km at $\lambda = 1550$ nm), all of which fit the assumptions made for Eq. (1). These parameters result in a differential wave-vector mismatch (obtained from the measured group-index birefringence of

#106045 - $15.00 USD Received 6 Jan 2009; revised 23 Feb 2009; accepted 24 Feb 2009; published 3 Mar 2009

(a)

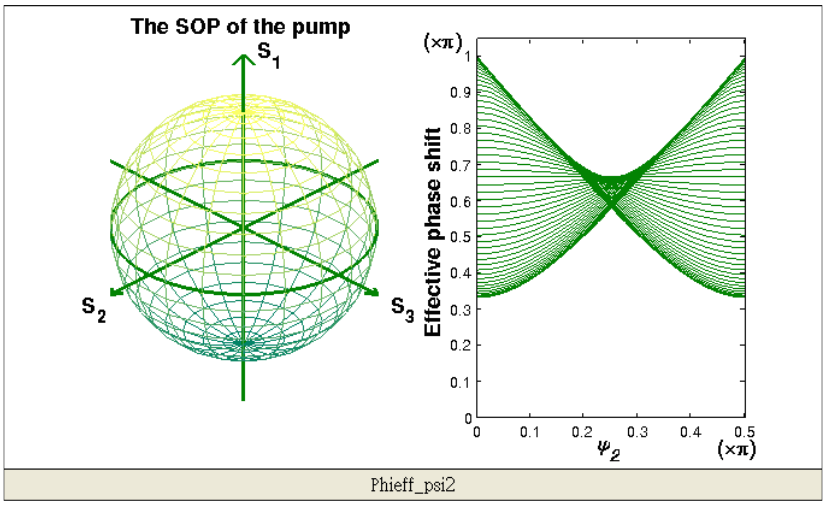


(b)

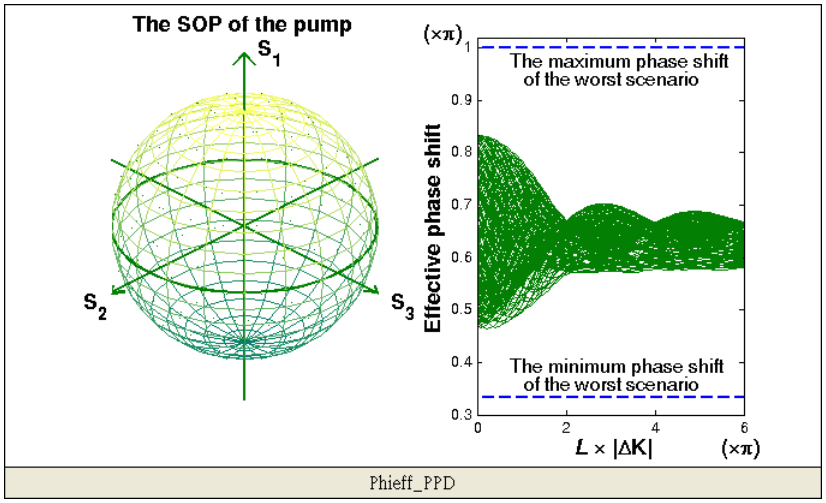


Fig. 2. With $\Phi = \pi$, (a) (Media 1)the effective phase shift with $L|\Delta K| >> 2\pi$ as a function of $\psi_2$, and (b) (Media 2) the effective phase shift for the best scenario ($\psi_2 = \pi/4$) as a function of $L|\Delta K|$.

the PCF [8]) given by

$$\Delta K = 1.02\times 10^6 \times (\frac{1}{\lambda_1} - \frac{1}{\lambda_2}) + 7.04\times 10^2 \times \ln\frac{\lambda_1}{\lambda_2}, \tag{13}$$

where $\Delta K$ is in 1/m and $\lambda$ is in nm. With both pump and probe wavelengths within the ITU-T C-band (1530-1565 nm) Eq. (13) approximates to $0.03\times\Delta\lambda$, so that a PPD greater than about 7 nm is required to attain polarization-insensitive operation. However, the PPD can be significantly reduced with a longer or a more birefringent PCF.

Figure 3 plots Eq. (12) for the maximum and minimum effective phase shifts versus $\Phi$ for several different values of $L|\Delta K|$ (as previously noted, the effective phase shift $\phi_{eff}$ fluctuates between two extremes termed the "maximum" and the "minimum" that

#106045 - $15.00 USD Received 6 Jan 2009; revised 23 Feb 2009; accepted 24 Feb 2009; published 3 Mar 2009

generally depend on launch conditions.) Once again, $\psi_2 = \pi/4$ is termed the best scenario, while $\psi_2 = 0$ (or $\pi/2$), the worst scenario. Figure 3 reveals that the phase shifts for the best

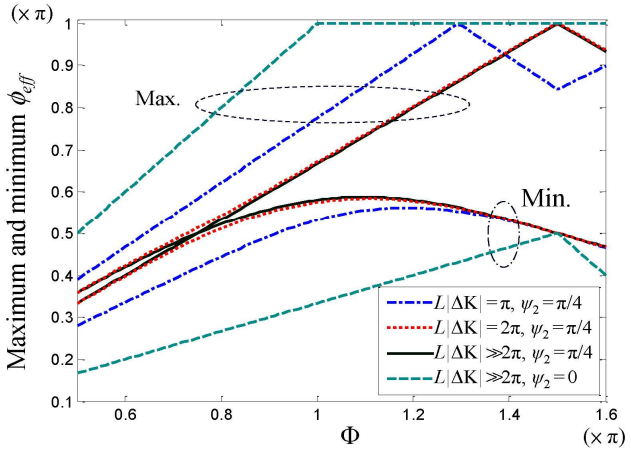


Fig. 3. Maximum and minimum effective phase shifts as functions of $\Phi$ (Eq. (12)).

scenario with $L|\Delta K| = 2\pi$ and $L|\Delta K| >> 2\pi$ are about the same. Fig. 3 also demonstrates that a polarization-independent phase shift can be attained by making $\psi_2 = \pi/4$, $\Phi = 3\pi/4$ and $L|\Delta K| >> 2\pi$, although the resultant effective phase shift is only $0.5\pi$ (which can alsobe derived using Eq. (12)). However, to optimize the minimum phase shift to $\phi_{eff} \sim 0.59\pi$ for the best scenario, $\Phi = 1.1\pi$ will be required. Additionally, to achieve the largest minimum phase shift for the worst scenario, $\Phi = 1.5\pi$ will be required and that phase shift is only $0.5\pi$. Moreover, at $\Phi = 1.5\pi$, the effective phase shift expressed by Eq. (12) reduces to $\pi - \pi|\cos(2\psi_1)|/2$, which is independent of $\psi_2$.

### 3. Penalty induced by insufficient phase shift

After understanding the polarization-dependent phase shift, it is necessary to investigate how the receiver performance of the converted RZ-BPSK signal is affected by insufficient XPM-induced nonlinear phase shift ($< \pi$). To simplify the discussion, the induced nonlinear phase shift over the entire pulse is set constant assuming that the pump pulses are significantly broader than the probe pulses: for instance, the pump pulse was almost three-times larger than the probe pulse in an earlier work [8]. Additionally, if an optical matched filter is used preceding the receiver, the pulse shape of the RZ-BPSK signal will not affect the discussion. Further, the RZ-BPSK probe $\mathbf{E}(t) = E_x(t)\hat{\mathbf{x}} + E_y(t)\hat{\mathbf{y}}$ is equivalent to either $\mathbf{A}_2(L)$ or $\mathbf{A}_2(0)$, depending on whether the RZ-OOK pump beam is a mark or a space. Considering a system limited by amplified spontaneous emission (ASE) noise, the received RZ-BPSK signal can be represented as $\mathbf{E}_r(t) = (E_x(t) + n_x(t))\hat{\mathbf{x}} + (E_y(t) + n_y(t))\hat{\mathbf{y}}$ [11]. The ASE noise components $n_x$ and $n_y$ are independent, identically distributed (i.i.d.) complex zero-mean circular Gaussian random variables (GRVs), and the variances of the real and imaginary parts of the noise components are identically $\sigma_n^2$, i.e. $\langle |n_x|^2 \rangle = \langle |n_y|^2 \rangle = 2\sigma_n^2$, where $\langle \cdot \rangle$ indicates the expectation value. At the output of the one-bit-delay interferometer, in which the RZ-BPSK signal interferes with its delayed replica, the output duobinary (DB) and alternate-mark inversion (AMI) signals respectively are $(\mathbf{E}_r(t) + \mathbf{E}_r(t-T))/2$ and $(\mathbf{E}_r(t) - \mathbf{E}_r(t-T))/2$.

#106045 - $15.00 USD Received 6 Jan 2009; revised 23 Feb 2009; accepted 24 Feb 2009; published 3 Mar 2009

Setting the detector responsivity to unity, the DB and AMI photocurrents of the detectors are represented as,

$$i_{DB}(t)=\sum_{p=x,y}\left|\frac{E_p(t)+E_p(t-T)}{2}+\frac{n_p(t)+n_p(t-T)}{2}\right|^2, \tag{14}$$

$$i_{AMI}(t)=\sum_{p=x,y}\left|\frac{E_p(t)-E_p(t-T)}{2}+\frac{n_p(t)-n_p(t-T)}{2}\right|^2. \tag{15}$$

Because the real and imaginary parts of all $\left[n_p(t)\pm n_p(t-T)\right]/2$ combinations are still i.i.d. GRVs with variances of $\sigma_n^2/2$, normalizing the photocurrents by $\sigma_n^2/2$ results in $\chi^2$ distributions with four degrees of freedom and a non-centrality parameter of [12],

$$\xi=\sum_{p=x,y}\frac{\left|E_p(t)\pm E_p(t-T)\right|^2}{2\sigma_n^2}. \tag{16}$$

Accordingly, the probability density functions (p.d.f.) of the normalized photocurrents $v=i/|\mathbf{A}_2|^2$ are [12],

$$p_V(v)=4\rho_s\sqrt{\frac{\rho_s v}{\xi}}\,e^{-2\rho_s v-\frac{\xi}{2}}I_1\left(2\sqrt{\xi\rho_s v}\right) \tag{17}$$

where $\rho_s=|\mathbf{A}_2|^2/(2\sigma_n^2)$ is the signal-to-noise ratio (SNR), and $I_1(x)$ is the first-order modified Bessel function of the first kind. For the in-phase case (denoted by $V^{in}$), both of $\mathbf{E}(t)$ and $\mathbf{E}(t-T)$ are equal to either $\mathbf{A}_2(0)$ or $\mathbf{A}_2(L)$, and the non-centrality parameters become $\xi=4\rho_s$ for the DB signal and $\xi=0$ for the AMI signal. Therefore, the corresponding p.d.f.s are,

$$p_{V_{DB}^{in}}(v)=2\rho_s\sqrt{v}\,e^{-2\rho_s(1+v)}I_1\left(4\rho_s\sqrt{v}\right), \tag{18}$$

$$p_{V_{AMI}^{in}}(v)=4\rho_s^2 v\,e^{-2\rho_s v}, \tag{19}$$

Furthermore, if either one of $\mathbf{E}(t)$ and $\mathbf{E}(t-T)$ is $\mathbf{A}_2(0)$ and the other is $\mathbf{A}_2(L)$ for the out-of-phase case (denoted by $V^{out}$), the non-centrality parameters become $\xi=4\rho_s\cos^2\left(\phi_{eff}/2\right)$ for the DB signal and $\xi=4\rho_s\sin^2\left(\phi_{eff}/2\right)$ for the AMI signal, and the p.d.f.s of the normalized photocurrents become

$$p_{V_{DB}^{out}}(v)=2\rho_s\sqrt{v}\sec\left(\frac{\phi_{eff}}{2}\right)e^{-2\rho_s\left[\cos^2\left(\frac{\phi_{eff}}{2}\right)+v\right]}I_1\left(4\rho_s\sqrt{v}\cos\left(\frac{\phi_{eff}}{2}\right)\right), \tag{20}$$

$$p_{V_{AMI}^{out}}(v)=2\rho_s\sqrt{v}\csc\left(\frac{\phi_{eff}}{2}\right)e^{-2\rho_s\left[\sin^2\left(\frac{\phi_{eff}}{2}\right)+v\right]}I_1\left(4\rho_s\sqrt{v}\sin\left(\frac{\phi_{eff}}{2}\right)\right), \tag{21}$$

where the definition of $\phi_{eff}$ is given by Eq. (11). Because Eqs. (18)-(21) are mutually independent, and $i_{DB}(t)-i_{AMI}(t)$ is used to determine the logic of the received RZ-BPSK

#106045 - $15.00 USD Received 6 Jan 2009; revised 23 Feb 2009; accepted 24 Feb 2009; published 3 Mar 2009

signal, the error probabilities are $p_e^{in} = \left\langle V_{DB}^{in} - V_{AMI}^{in} < h \right\rangle$ and $p_e^{out} = \left\langle V_{DB}^{out} - V_{AMI}^{out} > h \right\rangle$, where $h$ is the normalized receiver threshold, and $h = 100\%$ indicates the threshold is equal to $|\mathbf{A}_2|^2$. Note that as $\phi_{eff} < \pi$ only affects $V_{DB}^{out}$ and $V_{AMI}^{out}$, $h \geq 0$ is assumed here. Following Stein [13] and Ho [14], the analytical forms of error probabilities can be derived as

$$p_e^{in} = 1 - Q_1\left(2\sqrt{\rho_s}, 2\sqrt{\rho_s h}\right) + \frac{1}{2} e^{-\rho_s + 2\rho_s h} Q_1\left(\sqrt{2\rho_s}, 2\sqrt{2\rho_s h}\right) \tag{22}$$
$$- \frac{1}{8} e^{-2\rho_s - 2\rho_s h} \sqrt{h}\, I_1\left(4\rho_s \sqrt{h}\right) + \frac{1}{8} e^{-2\rho_s - 2\rho_s h} \sum_{n=1}^{\infty} n \left(2\sqrt{h}\right)^{-n} I_n\left(4\rho_s \sqrt{h}\right),$$

$$p_e^{out} = e^{-\rho_s(1+2h)} \sum_{n=0}^{\infty} \left( a_n - 4a_{n-1} - a_{n-2} + 8 \sum_{m=0}^{n-1} a_m \right) \times \cot^{n-1}\left(\frac{\phi_{eff}}{2}\right) I_{n-1}\left(\rho_s \sin\left(\frac{\phi_{eff}}{2}\right)\right),$$

$$= e^{-\rho_s\left[1+\cos^2\left(\frac{\phi_{eff}}{2}\right)+2h\right]} \sum_{n=0}^{\infty} \left( \tilde{a}_n + 4 \sum_{m=0}^{n-1} \left(2^{n-m} - 1\right) \tilde{a}_m - \sum_{m=1}^{n-1} \sum_{m'=0}^{m-1} \tilde{a}_{m'} \right)$$
$$\times \left( \frac{\cos\left(\frac{\phi_{eff}}{2}\right)}{2\sqrt{h}} \right)^{n-1} I_{n-1}\left(4\rho_s \cos\left(\frac{\phi_{eff}}{2}\right)\right), \tag{23}$$

where

$$a_m = \frac{1}{8}\delta_{0,m} + \frac{1}{8} \sum_{l=1}^{m} \frac{(-1)^{n-l}}{l!} \binom{m-1}{l-1} (4\rho_s h)^l, \tag{24}$$

$$\bar{a}_m = \frac{1}{8}\delta_{0,m} + \frac{1}{8} \sum_{l=1}^{m} \frac{1}{l!} \binom{m-1}{l-1} \left(\rho_s \sin^2\left(\frac{\phi_{eff}}{2}\right)\right)^l, \tag{25}$$

$Q_1(\alpha, \beta)$ is the first-order Marcum Q-function; $\binom{n}{k}$ is the binomial coefficient, and $\delta_{m,n}$ is the Kronecker delta function. Equations (22) and (23) are equivalent, but they are numerically efficient for respectively low and high thresholds. If the in-phase and out-of-phase cases are *equally* probable, the total error probability is then $p_e = (p_e^{in} + p_e^{out})/2$. Recall that the fixed threshold of zero for an ideal DPSK signal is one of its advantages, compared with the SNR-dependent threshold of an RZ-OOK signal. For the converted RZ-BPSK signal however, the optimal threshold is not zero for $\phi_{eff} < \pi$, and can be obtained by setting $(dp_e/dh)|_{h=h_{opt}} = 0$. Furthermore, $h_{opt}$ could be approximated as $\bar{h}_{opt} = (\langle V_{DB}^{in} - V_{AMI}^{in} \rangle - \langle V_{DB}^{out} - V_{AMI}^{out} \rangle)/2$ $= \cos^2(\phi_{eff}/2)$ assuming that the in-phase and out-of-phase distributions are symmetric.

The exact and approximated optimal thresholds are depicted in Fig. 4(a). In fact, $h_{opt}$ is SNR-dependent, and those plotted in Fig. 4(a) correspond to sensitivities (SNR required to reach the error probability $10^{-9}$), which are plotted in Fig. 4(b). The maximum sensitivity

#106045 - $15.00 USD Received 6 Jan 2009; revised 23 Feb 2009; accepted 24 Feb 2009; published 3 Mar 2009

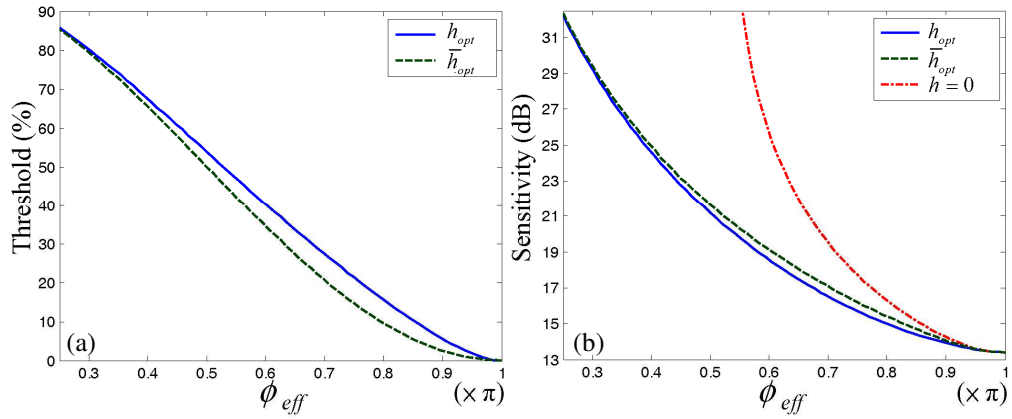


Fig. 4. (a) The optimal thresholds, and (b) the sensitivities as functions of $\phi_{eff}$ .

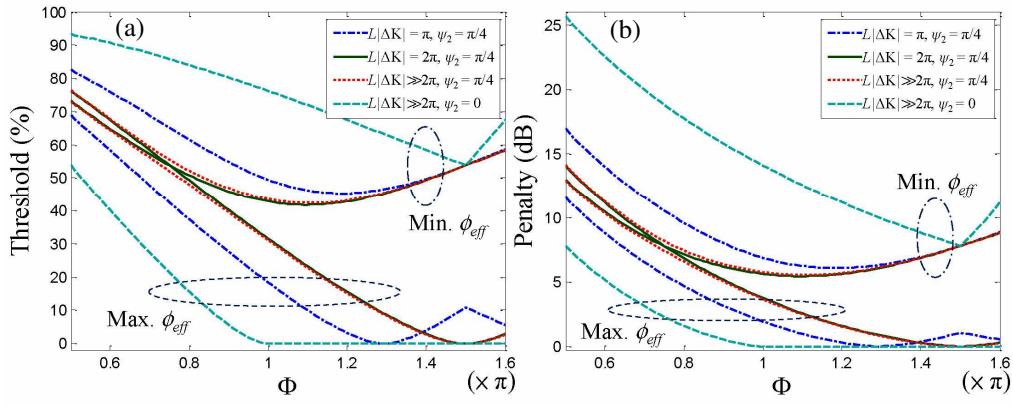


Fig. 5. (a) The optimal thresholds, and (b) the sensitivity penalty as functions of Φ .

difference between using $h_{opt}$ and $\bar{h}_{opt}$ is only about 0.7 dB indicating that the approximation is acceptable. The case of zero threshold is also shown for comparison, for which the RZ-BPSK signal cannot achieve error free reception for $\phi_{eff} < \pi/2$ . The optimal thresholds and the penalties in receiver sensitivity (relative to ideal or baseline RZ-BPSK) as functions of Φ are plotted in Fig. 5 according to Figs. 3 and 4, where both cases of the maximum and the minimum $\phi_{eff}$ are shown to illustrate the fluctuations in threshold and sensitivity penalty as the pump SOP is varied. For the worst scenario with $L|\Delta K| >> 2\pi$ , and $\Phi = \pi$ (which yields a $\phi_{eff}$ fluctuation of π - π/3 from Fig. 3 as the pump SOP is swept over the Poincaré sphere), the resultant threshold and sensitivity penalty of the RZ-BPSK probe respectively fluctuate as 0 - 76.2%, and 0 - 14 dB; but those fluctuations are respectively mitigated to 0 - 53.8% and 0 - 7.8 dB by setting $\Phi = 1.5\pi$ . By contrast, for the best scenario with $L|\Delta K| >> 2\pi$ and $\Phi = \pi$ (which yields a $\phi_{eff}$ fluctuation of ~ 0.67π - 0.58π from Fig. 3 as the pump SOP is swept over the Poincaré sphere), the respective threshold and sensitivity penalty fluctuations reduce to 31.5 - 42.8% and 3.7 - 5.6 dB. Thus, launching the probe at $\pi/4$ with $L|\Delta K| \geq 2\pi$ and a fixed Φ can decrease the fluctuations of both threshold and sensitivity caused by an arbitrarily polarized RZ-OOK pump, but the penalty is never zero. Moreover, for perfect polarization-independent operation ( $\psi_2 = \pi/4$ , $\Phi = 3\pi/4$ and $L|\Delta K| >> 2\pi$ in Fig. 3), the phase shift is always only $\pi/2$ , and the sensitivity penalty is 7.8 dB (relative to ideal RZ-

#106045 - $15.00 USD Received 6 Jan 2009; revised 23 Feb 2009; accepted 24 Feb 2009; published 3 Mar 2009

BPSK) which agrees well with the experimental value of ~ 7 dB [8]. For this case, it implies that RZ-BPSK requires higher SNR to achieve an error probability compared with ideal RZ-OOK due to different statistics, even though their symbol distances on the constellation diagram are the same (since the phase shift for RZ-BPSK is only $\pi/2$ for polarization-independent operation).

## 4. Conclusion

This work theoretically analyzes the XPM effect for RZ-OOK-to-BPSK format conversion in a highly birefringent HNLF with an arbitrary polarized RZ-OOK pump beam. The nonlinear phase-shift-dependent receiver sensitivity and threshold of the resultant RZ-BPSK signal are also derived analytically for the first time. When the XPM-induced nonlinear phase shift $\Phi$ is set to $\pi$ at large ( $L|\Delta K| >> 2\pi$ ) PPD, the probe's effective phase shift $\phi_{eff}$ will fluctuate between $\pi$ and $\pi/3$ once the pump SOP begins to sweep the Poincaré sphere. For this scenario, the corresponding sensitivity (SNR required to reach the error probability $10^{-9}$ ) penalty and threshold (normalized to $|\mathbf{A}_2|^2$ ) of the RZ-BPSK probe fluctuate as 13.4 - 27.5 dB and 0 - 76.2% respectively. By contrast, although launching the probe at $\pi/4$ relative to the birefringent axes with sufficient PPD ( $L|\Delta K| \geq 2\pi$ ) and $\Phi = \pi$ may not achieve the desired $\pi$ effective phase shift, it can reduce the respective fluctuations in sensitivity penalty and threshold to 3.7 - 5.6 dB and 31.5 - 42.8%.

#106045 - $15.00 USD Received 6 Jan 2009; revised 23 Feb 2009; accepted 24 Feb 2009; published 3 Mar 2009